

Article

Branch Occlusion and Discoloration under the Natural Pruning of *Mytilaria laosensis*

Guoming Qin ^{1,2}, Jian Hao ³, Jinchang Yang ¹, Rongsheng Li ¹ and Guangtian Yin ^{1,*}

¹ Research Institute of Tropical Forestry, Chinese Academy of Forestry, Guangzhou 510520, China; qgm_092@163.com (G.Q.); fjjc168@126.com (J.Y.); fjlr_123@126.com (R.L.)

² Institute of Forestry, Nanjing Forestry University, Nanjing 210037, China

³ Experimental Center of Tropical Forestry, Chinese Academy of Forestry, Pingxiang, Guangxi 536000, China; pxhj88@126.com

* Correspondence: yinguangtian@126.com; Tel.: +86-136-0288-0169

Received: 29 August 2019; Accepted: 6 October 2019; Published: 9 October 2019



Abstract: The production of knot-free and high-quality wood can be a vital issue in silviculture and forest management. In this study, knot properties, branch occlusion, and wood discoloration were investigated in an 11-year-old *Mytilaria laosensis* plantation in Guangxi, China, to examine the effectiveness of natural pruning in reducing knot-related defects. A total of 1513 occluded branches from 20 trees were sampled and dissected. Occluded branches were most common at heights of 2–6 m, and the mean diameter of the occluded branches gradually increased with height from the base to 6 m. Linear and generalized linear mixed-effect models were developed to reveal the relationship between branch occlusion and discoloration. The mortality of branches was highest in the third and fourth year and it took roughly three to six years to occlude. The mixed-models indicated that the branch occlusion time was positively correlated with the occluded branch diameter and dead branch stub length, and negatively correlated with the stem radial increment during branch occlusion. Branch discoloration was positively correlated with the occluded branch diameter and branch occlusion time, and was negatively correlated with the branch angle. The probability of wood discoloration also increased with the branch occlusion time. Our findings contribute to a better understanding of the spatiotemporal allocation and internal characteristics of occluded branches, and provide a reference for growing high-quality *M. laosensis* wood.

Keywords: knot properties; wood defects; clear wood; mixed model

1. Introduction

Regulating the development of tree crowns and their branches is an important method of forest management to promote tree growth. Silvicultural interventions such as pruning and thinning are commonly applied to improve timber quality and tree growth [1,2]. Nevertheless, the branches constituting the tree crown are also important for the inner structure of the stem [3,4]. Branch development can result in knot-related defects on the wood.

Knots are the primary cause of defects in log grading [5], and can be divided into live (sound) and dead (decaying) knots, where live knots are intergrown with the wood, unlike dead knots, which are encased. Knot-related defects mainly result from the decaying portion of knots caused by fungal infections, and greatly affect the appearance, quality, and mechanical properties of the wood [6–8], which are important indices in timber grading evaluation. Hence, exploring methods for minimizing the occurrence of dead knot-related defects has become an essential research topic.

To date, only a few studies have analyzed knot-related properties after natural pruning for broadleaved species [9–11]. The studies of Hein on *Fraxinus excelsior* and *Acer pseudoplatanus* showed

that occluded branch diameters and the mean stem radial increment played vital roles in predicting knot characteristics [12]. The duration of branch occlusion was also found to be strongly related to the branch dimension [13]. Decay or discoloration was significantly correlated with the occluded branch diameter, dead branch stub length, and duration of branch occlusion [14]. Nevertheless, there are few published studies on the relationships between branch occlusion, knot characteristics, and wood discoloration for valuable tropical and subtropical tree species.

Mytilaria laosensis Lecomte is a valuable broad-leaved tree species that is mainly distributed in the tropical and subtropical areas of Southeast Asia and south China [15,16]. *M. laosensis* has been widely used in the establishment of fast-growing and high-yield plantations owing to its high productivity, exceptional quality, and attractive wood grain. Furthermore, these trees have evident impacts on many environmental factors, such as soil and water conservation, and contribute to soil improvement [17]. However, due to the large amount of branches, as well as weak natural pruning, the timber of *M. laosensis* greatly suffers from knot-related defects [18] (Figure 2), and information on forest management methods to reduce these defects in this species is lacking.

The overall goals of this study were to (i) identify the spatial distribution of occluded branches and the process of occlusion at different ages in an *M. laosensis* plantation, (ii) model the relationships between the main branch properties of *M. laosensis*, and (iii) predict the extent of branch discoloration on the stem and the probability of wood discoloration. These results should contribute to a deeper understanding of the characteristics of occlusions in *M. laosensis*, and provide silvicultural guidance for the cultivation of *M. laosensis* and other valuable timber species.

2. Material and Methods

2.1. Experimental Site

The study site is located at Qingshan Forest Farm, Experimental Center of Tropical Forestry, Pingxiang City, Guangxi Zhuang Autonomous Region, China (22°02′–22°19′ N, 106°43′–106°52′ E) (Figure 1). This site has a subtropical climate, with obvious dry and wet seasons. The annual average temperature is about 19.5 °C–21.4 °C, with a maximum of 38.7 °C and a minimum of −1.5 °C. Annual precipitation is about 1210 mm, and is concentrated from April to October. The plantation is on a south-facing slope, with a mean altitude of 440 m. The soils at the study site are categorized as red soils from siliceous rock. The former planting species of this site was *Cunninghamia lanceolata* (Lamb.) Hook. Being planted in 1977, this forest had an initial planting density of 10,000 trees/hm², which was thinned to 6667 trees/hm² in 1987, and finally harvested in 2006. No fertilization was applied in this plantation.

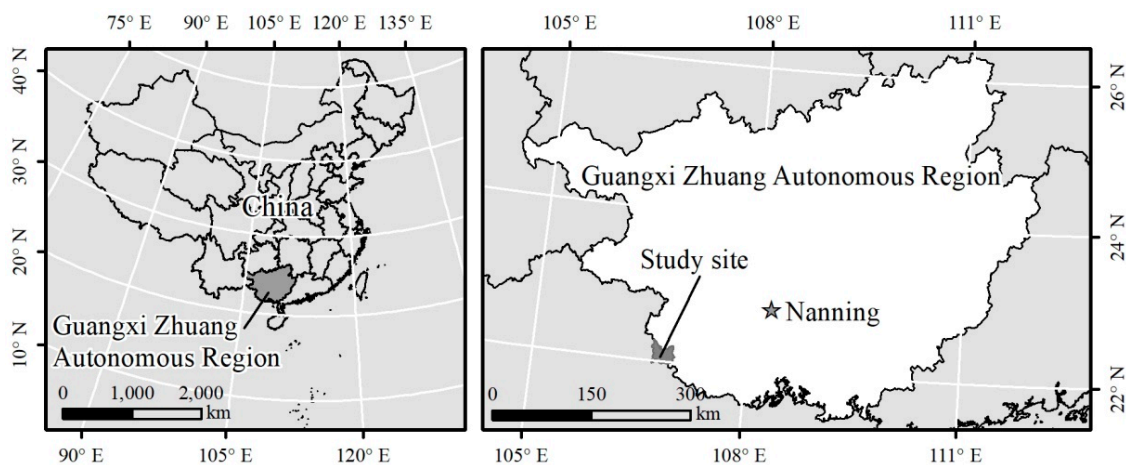


Figure 1. The location of the study site.

2.2. Measurements

M. laosensis seedlings were planted in 2008, with an initial planting density of 1667 stems per hectare (2 m × 3 m spacing). Five plots (20 m × 30 m) were randomly selected in the forests for evaluation. No thinning or fertilization had been conducted at this site. In February 2019, each tree was measured in all five plots; abbreviations of measurement variables and their units are listed in Table 1. Following measurement, four dominant or co-dominant trees were selected and felled by a chainsaw for the data analysis per plot. The height of the tree, diameter at breast height (DBH), height of the lowest living branch, and crown width of these trees were measured in the 11-year-old *M. laosensis* plantation (Table 2); a total of 20 trees in each plot were selected for felling and measurement. After the tree was felled, the number and height of all the occluded branches on the stem were numbered and counted. Because smaller branches have little influence on the growth and quality of trees, and the knots that form after the development of smaller branches are difficult to judge from their appearance alone, branches with a diameter of less than 5 mm were not counted (Figure 2). Stem sections of about 20–30 cm length with completely occluded branches were cut with a chainsaw. If there were multiple occluded branches in different directions at the same height, the larger-diameter segments were selected for retention. Each disc was then ground with an electric sander with 120-grit sandpaper, and the angle between each occluded branch and the north on the surface of the disc was marked (using a pencil) as the azimuth. Finally, a band saw was used to longitudinally dissect along the center of the occluded branches or the core of the branches, and the split surface with the complete knot structure was polished with a polisher. A total of 1513 occluded branch samples were obtained for the measurement and analysis (Table 3).

Table 1. Variable abbreviations.

Variables	Definition	Unit
Tree-level variables		
H	Tree total height	(m)
DBH	Diameter at breast height	(cm)
HCB	Height of the crown base	(m)
CD	Diameter of the crown	(m)
Branch-level variables		
EA	Branch exertion angle	(°)
BH	Branch height on stem	(m)
YD	Year of branch death	(year)
YO	Year of branch complete occlusion	(year)
OT	Branch occlusion time	(year)
IROT	Mean stem radial increment during the branch occlusion	(mm/year)
OB	Occluded branch	
OBD	Occluded branch diameter	(mm)
CT	Cork tissue (0 = absent, 1 = present)	
DBSL	Dead branch stub length	(mm)
DL	Discoloration length	(mm)
DSW	Discoloration in stem wood (0 = absent, 1 = present)	
Model descriptors		
a, b, c	Coefficient of fixed effect	
t, tb	Subscripts for tree, branch	
α, β, γ	Coefficient of random effect	
Ln ()	Natural log-link	
RMSE	Root mean squared error	
$R^2_{(c)}$. $R^2_{(m)}$	Conditional and marginal R^2	

Table 2. Summary tree statistics.

Variables	Unit	Minimum–Maximum	Mean
Tree total height	m	16.4–22.8	19.3
Diameter at breast height	cm	17.2–25.3	21.1
Height of the live crown base	m	4.2–8.8	6.8
Diameter of the crown	m	6.5–10.4	8.6

**Figure 2.** The dead branches below the live crown of a standing *Mytilaria laosensis* (a); the appearance of the occluded branch (b); the longitudinal section of an occluded branch (c).**Table 3.** Summary individual-branch statistics.

Variables (Abbreviation)	Unit	Minimum–Maximum	Mean
Branch exertion angle (EA)	(°)	3.9–98.5	54.1
Branch height on the stem (BH)	(m)	0.1–18.8	9.5
Year of branch death (YD)	(year)	2–8	2.6
Branch occlusion time (OT)	(year)	1–10	4.6
Mean stem radial increment during branch occlusion (IROT)	(mm/year)	1.3–55	11.1
Occluded branch diameter (OBD)	(mm)	4.7–59.1	23.7
Dead branch stub length (DBSL)	(mm)	6.1–148.5	47.2
Discoloration length (DL)	(mm)	17.2–193.3	100.3
Discoloration in stem wood (DSW)		0–1	0.09

The internal occluded branch and knots were measured according to the method described by Hein [1]. For the specimen, the year of death (YD) of the branch is calculated as the average between the first year in which the branch begins to occlude and the last year in which the dead branch stub persists. The year of branch occlusion (YO) is the year in which the stub is completely covered by the new annual ring. The branch occlusion time (OT) is the duration from the year of death of the branch to the year of branch occlusion, calculated as the difference between the year of branch closure and the year of branch death. The occluded branch diameter (OBD) refers to the maximum width of the branch (M–K in Figure 3). For natural pruning, we defined a dead branch as part of the branch stub, i.e., the part that has been significantly spoiled and not connected to the surrounding rings [1]. The branch discoloration length (DL) was measured along the branch pith (J–P in Figure 3). The branch exertion angle (EA) was defined as the upward angle between the pith of the stem and the pith of the

branch ($\angle GNJ$ in Figure 3). The dead branch of stub length (DBSL) was measured along the direction of the stem radius (C–F in Figure 3). Regarding the existence of dead knots and wood discoloration, we referred to Danescu’s research method [19]. In brief, we recorded whether there was cork tissue (CT) inside the knot, covering part of the surface of the branch, and formed by part of the callus; this was recorded as present or not. In addition, we recorded whether these discolored parts spread from the branches to the center of the stem (DSW); if the discolored part of the branch extended from the branches to the stem, it was judged to be discolored. The stem radial increment during branch occlusion (IROT) was measured at the point where the stem was uniform, without any bulge.

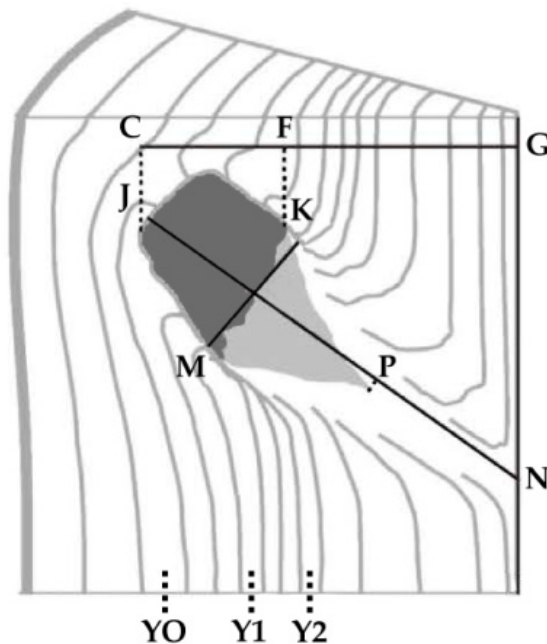


Figure 3. Longitudinal section of the occluded branch after natural pruning (modified from Hein [1]). $MK = OBD$; $JP = DL$; $CF = DBSL$; $\angle GNJ = EA$; $YD = (Y1 + Y2)/2$, in which $Y1$ is the first year of branch occlusion and $Y2$ is the last year of branch growth. The dark gray portion shows the decayed part under a naturally pruning branch. OBD: occluded branch diameter; DL: branch discoloration length; DBSL: dead branch of stub length; EA: branch exertion angle; YD: year of branch death; YO: year of branch occlusion.

2.3. Statistical Analysis

Since the data collected included continuous variables (e.g., DL, DBSL, and OBD), count variables (e.g., YD, YO, and OT), and binary variables (e.g., DSW), different models were applied. Continuous variables were analyzed with linear mixed-effects models (LMMs), where random effects and residuals were assumed to obey a normal distribution. Count variables and binary variables were modeled using generalized linear mixed effects models (GLMMs). If the data were skewed, logarithmic transformation was performed before modeling. The data also had a hierarchical structure; that is, the branches were nested within the trees, and the trees were nested within the plots. Our LMM and GLMM models accounted for this nested structure by including plots, trees nested within plots, and branches nested within trees in the models.

The fixed and random effects were all tested using likelihood ratio tests when applying the restricted maximum likelihood estimation. To reveal the potential relationships between the occluded branch properties, OT, DBSL, EA, DL, and DSW were selected as response variables. The independent fixed variable, as well as random effects, such as plots, trees, and branches, were tested. Variables with a biologically plausible interpretation were included in the models at the significance ≤ 0.01 . The optimal equations were selected through the principle of minimizing Akaike’s Information Criterion and Bayesian’s Information Criteria [20]. When fitting the models, the predictors were all diagnosed with

variance inflation factors (VIF) [21]. In the process of selecting variables, independent variables with VIF values above 5 were considered to be collinear. The stepwise regression was used to determine the independent variables when they were collinear.

To evaluate the model's performance, we used the root mean squared error (RMSE) to test the constructed model against the original data. For the GLMMs and LMMs, the marginal $R^2_{(m)}$ (including the fixed effect) and the conditional $R^2_{(c)}$ (including both the fixed effect and the random effect) were used to examine the performance of the model [22]. For the binomial-GLMMs, we used the area under curve (AUC) value [23] to evaluate the model fit. All models were developed using SPSS 21.0 (IBM-SPSS Inc., Chicago, IL, USA).

3. Results

3.1. Spatial Distribution of Branch Occlusions

The number of occluded branches in the stem of *M. laosensis* initially increased and then decreased with increasing tree height, and then tended to level out (Figure 4). Specifically, the number of occluded branches reached a maximum at 3 m, and then tended to level out from 8 m to the top of the tree. The stem section from a height of 2 m to 6 m accounted for more than 30% of the total number of occluded branches. The average diameter of knots increased gradually from the base of the stem to a maximum at 6 m, after which the knot size tended to plateau.

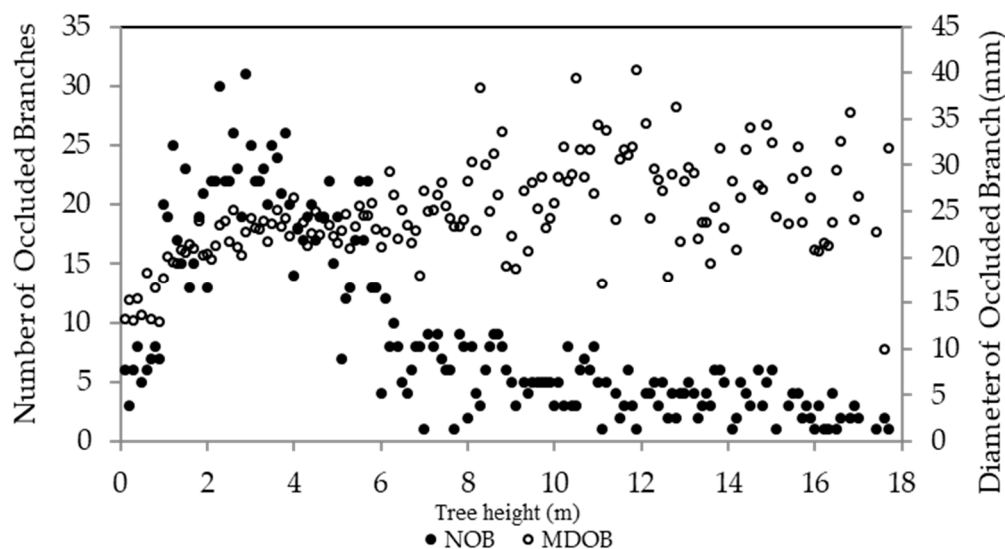


Figure 4. Distribution of occluded branches according to tree height (the whole dataset) with respect to the number of occluded branches (NOB) and mean diameter of occluded branches (MDOB). Plots were made at intervals of 0.1 m heights.

3.2. Temporal Distribution of Branch Occlusion

The distribution of the number of occluded branches of *M. laosensis* of different ages is shown in Figure 5. The majority of branches died in the first to second year of growth (52.6%), followed by the third to fourth year (39.31%), fifth to sixth year (5.56%), and seventh to eighth year of growth (1.46%). Years 5–6 and years 7–8 were the peak years for the completion of occlusion, accounting for about 87.17% of all occluded branches. The process of occlusion starts from the development of the branches and continues until the branch falls off, and the stem then grows over the wound. Most of the branches (76.65%) took about 3–6 years to occlude completely, and a small number took about 7–8 years to occlude.

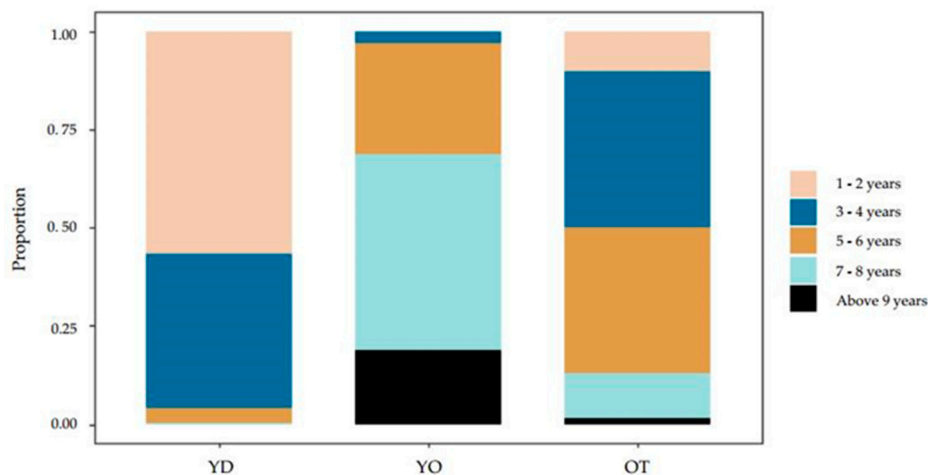


Figure 5. Temporal distribution of branch occlusion. YD and YO are the year of branch death and occlusion, respectively. OT is the time of branch occlusion.

3.3. Models for Branch Occlusion

3.3.1. Branch Occlusion Time

The GLMM was used to predict the occlusion of branches and the characteristics of knots. The branch occlusion time (OT) was estimated with a log-linear negative binomial. The fixed factors in the model were statically significant. No random effects were found to be statistically significant in Equation (1). The estimated value and standard error of fixed effects of Equation (1) are shown in Table 4. OT was significantly positively related to the occluded branch diameter (OBD) and dead branch stub length (DBSL), and negatively correlated with the mean IROT.

$$\ln(OT_{tb}) = a_0 + a_1 \times OBD_{tb} + a_2 \times DBSL_{tb} + a_3 \times IROT_{tb} \tag{1}$$

Therefore, Equation (1) demonstrates that the DBSL had a stronger relationship with OT than OBD had with OT (Figure 6a,b). The model explained half of the total variance ($R^2 = 56.29\%$; RMSE = 0.27 years).

Table 4. Estimated coefficients and standard errors for equations.

Equation	Response Variable	Parameters	Predictor Variable	Estimate	SE	$R^2_{(m)}$	$R^2_{(e)}$
Equation (1)	Branch occlusion time (OT) *	a_0	Intercept	1.361	0.037	56.29%	-
		a_1	OBD	0.022	0.003		
		a_2	DBSL	0.016	0.001		
		a_3	IROT	-0.062	0.004		
Equation (2)	Dead branch stub length (DBSL) *	a_0	Intercept	2.935	0.133	9.56%	-
		a_1	OBD *	0.226	0.039		
Equation (3)	Branch exertion angle (EA) *	a_0	Intercept	4.49	0.052	12.51%	16.94%
		a_1	OBD *	-0.174	0.015		
		γ_{pt}		0.013	0.005		
Equation (4)	Branch discoloration length (DL) *	a_0	Intercept	3.846	0.129	17.64%	26.17%
		a_1	OT	0.082	0.003		
		a_2	OBD *	0.312	0.016		
		a_3	EA *	-0.165	0.026		
		δ_{pt}		0.013	0.004		
Equation (5)	Probability of wood discoloration (DSW)	a_0	Intercept	-3.645	0.282	57.18%	81.54%
		a_1	OT	0.282	0.051		
		ϵ_{ptb}		0.012	0.004		

Note: * The variable was in logarithmic form in the equation. OBD: occluded branch diameter; DL: branch discoloration length; IROT: mean stem radial increment during branch occlusion; DBSL: dead branch of stub length; EA: branch exertion angle; OT: time of branch occlusion.

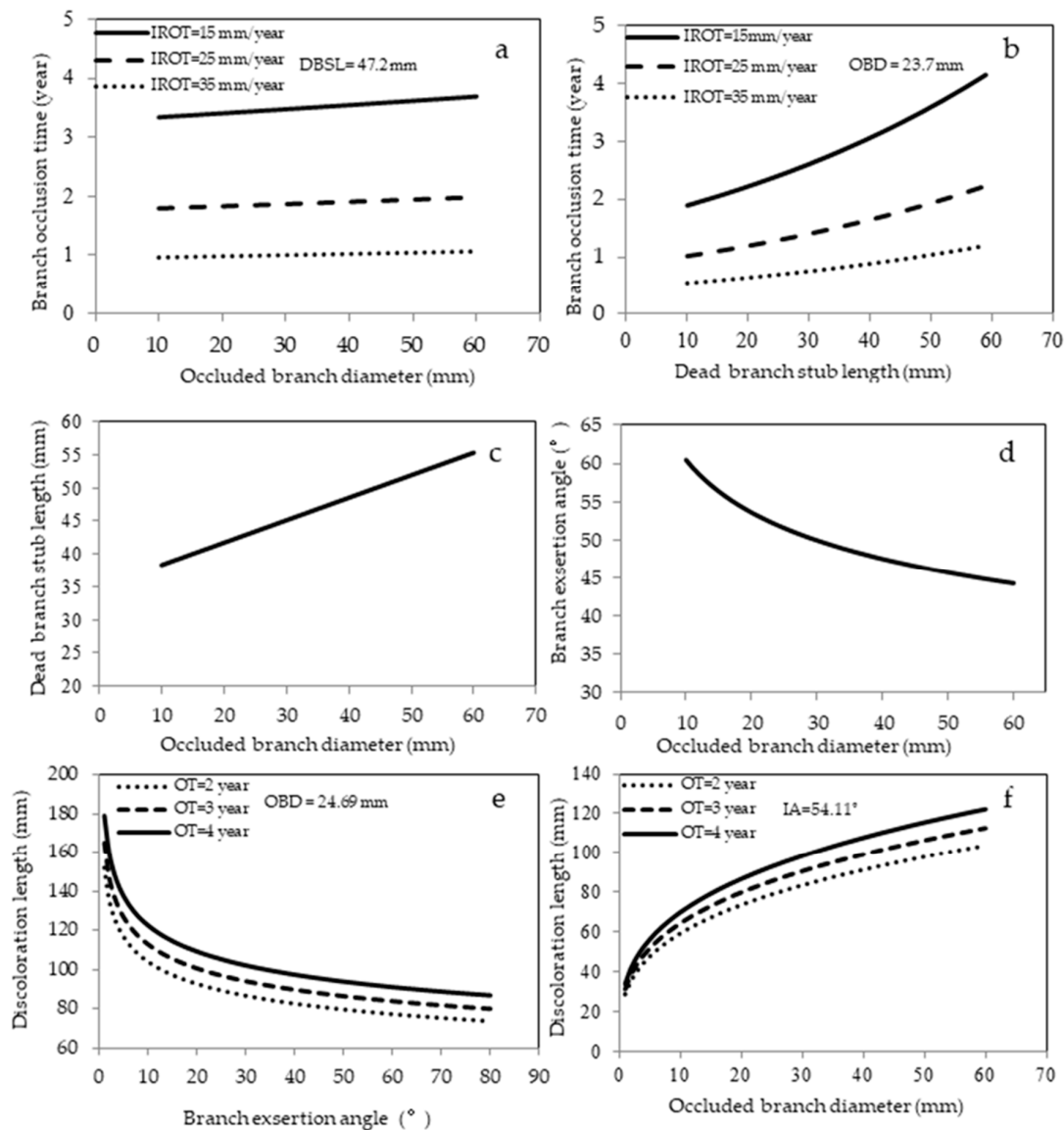


Figure 6. Simulation curves based on marginal models for predicting the branch occlusion time (a,b), dead branch stub length (c), branch exertion angle (d), and discoloration length (e,f). (a) Predicted branch occlusion time under natural pruning from the mean dead branch stub length of the whole dataset and different levels of mean stem radial increment during branch occlusion against the occluded branch diameter. (b) Predicted branch occlusion time from the mean occluded branch diameter and different levels of mean stem radial increment during branch occlusion against the dead branch stub length. (c) Predicted dead branch stub length against the occluded branch diameter. (d) Predicted branch exertion angle against the occluded branch diameter. (e) Predicted discoloration length from the mean occluded branch diameter and different levels of branch occlusion time against the branch exertion angle. (f) Predicted discoloration length from the mean branch exertion angle and different levels of branch occlusion time against the occluded branch diameter.

3.3.2. Dead Branch Stub Length

The model for DBSL was estimated with a log-link function with a normal distribution of errors. This model indicated that OBD was the only significant predictor (Equation (2)). The parameter estimates and standard errors of the equation are presented in Table 4.

$$\ln(\text{DBSL}_{\text{tb}}) = a_0 + a_1 \times \ln(\text{OBD}_{\text{tb}}) \tag{2}$$

This model showed that DBSL increased significantly with increasing OBD (Figure 6c). However, the model could only explain a very small amount of the total variation ($R^2 = 9.56\%$; RMSE = 20.89 mm).

3.3.3. Branch Exsertion Angle

The exsertion angle (EA) was estimated using a log-link function with a normal distribution of errors. The EA was correlated with log-transformed OBD. The estimates and standard error of the model and significant predictor are presented in Table 4.

$$\ln(EA_{tb}) = a_0 + a_1 \times \ln(OBD_{tb}) + \gamma_{pt} \quad (3)$$

Simulations with Equation (3) showed that EA decreased with increasing OBD (Figure 6d). The model explained only a small proportion of the total variation ($R^2_{(c)} = 16.94\%$; $R^2_{(m)} = 12.51\%$; RMSE = 7.22°).

3.3.4. Branch Discoloration Length

The discoloration length (DL) was modeled using a log-link function with a normal distribution of errors. DL was correlated with OT, OBD, and IA (Equation (4)). The factors involved in the model were all statistically significant. The parameter estimates and standard errors of the equation are presented in Table 4.

$$\ln(DL_{tb}) = a_0 + a_1 \times OT + a_2 \times \ln(OBD_{tb}) + a_3 \times \ln(IA_{tb}) + \delta_{pt} \quad (4)$$

The simulation plots of Equation (4) illustrated that the DBSL decreased with increasing EA, especially for branches less than 20° (Figure 6e). However, the DBSL increased with increasing OBD. This model could explain more than one quarter of the total variation ($R^2_{(c)} = 26.17\%$; $R^2_{(m)} = 17.64\%$; RMSE = 16.37 mm).

3.4. Wood Discoloration

The binomial-GLMM was used to determinate the discoloration of the stem. As shown in Equation (5), the possibility of discoloration of the wood (DSW) was significantly related to the branch OT (Figure 7). The parameter estimates and standard errors in the model are presented in Table 4.

$$\text{logit}(DSW_{tb}) = a_0 + a_1 \times OT + \varepsilon_{ptb} \quad (5)$$

Simulation of Equation (5) illustrated that as the OT increases, the possibility of wood discoloration also increases. The model performance was quite good ($R^2_{(c)} = 81.54\%$; $R^2_{(m)} = 57.18\%$; AUC = 0.932).

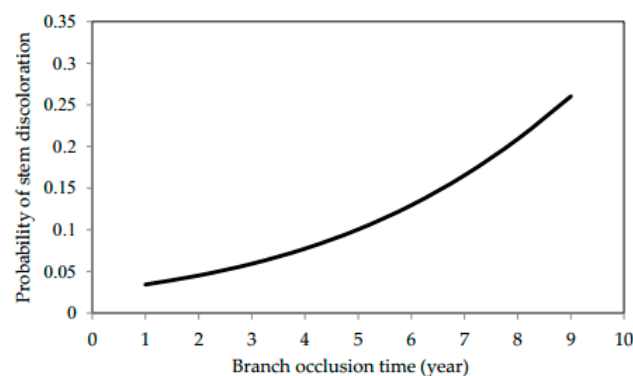


Figure 7. Predicted probability of wood discoloration for *M. laosensis* and the branch occlusion time.

4. Discussion

4.1. Branch Distribution

Knots were found to be mainly distributed on a tree at a height of 3–6 m; however, this is also the most valuable part of the tree. Moreover, the mean occluded branch diameter also showed an increasing trend for this part of the tree. This revealed that the most serious problem with the timber quality of *M. laosensis* is the knot size and amount, where knots have been identified as an important timber downgrading defect [24]. A previous study showed that a high planting density contributed to reducing the knot size [25]. This may have been due to the fact that high-density planting contributes to increases in competition between the trees and branches for limited growing space, water, and nutrients [26,27]. As the tree height increased above 6 m, the range of the average diameter of knots increased, and the coefficient of variation trend became stable. This is consistent with the results of Trincado's study of the branch properties of *Pinus taeda* [28]. A possible explanation for this pattern could be that as the depth of the tree crown increases, the interaction among the internal branches increases, resulting in an overall decrease in the diameter of the branches [26,29], which usually results in a small diameter range of branches within the tree crown.

Understanding temporal trends in branch and knot characteristics can help guide artificial pruning strategies. The current study showed that the mortality of branches was highest 3 to 4 years after planting. After the branches died and fell, dead branch stubs remained in the tree [30]. Our results showed that completion of the occlusion process requires about 5 to 6 years. Therefore, we can speculate that establishing the pruning period of *M. laosensis* within 4 to 6 years after planting may contribute to diminishing the formation of knot-related defects and result in a longer length of clear wood. In addition, the effects of different pruning intensities, pruning seasons, and pruning tools should also be considered [31,32].

4.2. Branch Occlusion Time

In this study, OT increased with increasing OBD and DBSL, and decreased with increasing IROT (Figure 6a,b). Similar results have been found for *Fraxinus excelsior* [33], *Acer pseudoplatanus* [33], *Quercus rubra* [34], and *Betula alnoides* [14]. We also found that DBSL was more closely related to OT than to OBD. These findings are in agreement with those of some studies on *Pseudotsuga menziesii* [35] and *Pinus ponderosa* [36]. However, Eq (2) showed a significant but weak relationship between OBD and DBSL. The reason for this may be that branch fractures are mostly caused by natural damage and accidental human damage, which leads to a wide range in the length of the dead stubs [1]. Consequently, OT could be reduced by pruning and other silvicultural measures. To reduce the DBSL and OBD, we can intensify competition in the forest, as more trees may reduce the growth of branches in a competitive environment. Wang et al. [25] studied the influence of different densities of *B. alnoides* and found that a high density can significantly reduce the diameter of branches. Furthermore, the stem diameter growth rate could be improved by fertilization and thinning [37,38]. Therefore, a combination of these measures will help to reduce the OBD and thus improve the stem diameter growth rate for the production of high-quality wood.

4.3. Branch Exsertion Angle

We further explored the relationship between EA and wood properties or other knot variables. EA showed a significant relationship with OBD: as the OBD increased, EA decreased (Figure 6d). A similar relationship was reported for several other hardwood species [11,12,14,33]. In addition, DL increased with decreasing EA. Beaulieu et al. [11] found that EA was mainly dependent on the age of the branch. However, this situation is more frequent in conifers, and is not as obvious for broadleaved trees [39]. In addition, EA and DL were found to be negatively correlated, which was especially evident when the EA was less than 20° (Figure 6e). Therefore, the DL of branches might be effectively reduced by increasing the EA [14]. However, the goodness of fit of the equation was low, indicating that there

were other unknown factors affecting EA, which could include tree variables such as branch position, crown structure, or genetic control [40]. This suggests that a combination of genetic improvement and forest management may contribute to the improvement of timber quality.

4.4. Discoloration

DL had a significant relationship with OT, OBD, and EA. Our model showed that DL was positively correlated with the OT and OBD, and was negatively correlated with EA, which was consistent with previous studies [14,19]. The present study revealed that a shorter OT for branches of the same size will be associated with a smaller DL, suggesting that faster occlusion contributes to reducing the size of branches, which will in turn diminish the risk of infections [6].

The ability of trees to resist the spread of decay will determine the overall degree of decay and quality of the wood [41,42]. A longer OT means longer wound exposure, and thus a greater risk of fungi infecting trees and invading the heartwood of the tree. In the current study, under natural pruning, there were only a few cases where wood discoloration was observed in *M. laosensis*. Danescu et al. [19] found that naturally shed branches did not cause any stem discoloration on *F. excelsior* L., whereas discoloration was observed on *A. pseudoplatanus*. Beadle et al. [43] also found discoloration on *Acacia mangium* under natural pruning. The difference in the susceptibility of different species to discoloration may be related to the chemical composition of the wood, type of fungi causing infection, site quality, environmental conditions [44–46], etc. The effects of pruning on *M. laosensis* and in response to different densities and management measures are topics worthy of further study.

5. Conclusions

We found that the number of occluded branches was greatest at stem heights of 2–6 m. For the 11-year-old trees examined in this study, the average diameter of knots increased gradually from the base of the stem to a maximum at 6 m. Pruning in the fifth to sixth year after planting will contribute to the production of longer lengths of knot-free wood. The simulation showed that bigger branches are significantly correlated with a longer branch occlusion time, longer discoloration length, larger dead branch stub, and steeper branch exertion. Our results suggest that accelerating the occlusion of branches will help to minimize the risk of wood discoloration. The occluded branch diameter and dead branch stub length were two fundamental indicators affecting timber quality. Artificial pruning can help to reduce the effects of dead branches. Further research is needed to investigate the effect of pruning and other silvicultural measures (e.g., planting density, fertilization, and thinning) on branch occlusion and thus the timber quality of *M. laosensis*.

Author Contributions: G.Y., J.H., and G.Q. designed the experiments; J.Y., R.L., and G.Q. performed the experiments; J.H. and G.Q. analyzed the data; G.Q. wrote the paper.

Funding: This study was financially supported by the Guangdong Forestry Science and Technology Innovation Project (2016KJ CX004) and the Science Foundation of Experiment Center of Tropical Forestry, Chinese Academy of Forestry (RL2011-04).

Acknowledgments: The authors thank Wenfu Guo, Baoguo Yang, and Weijun He for help with data collection. We also would like to thank Zeng Jie and Chunsheng Wang for their comments on this article. Sincere thanks to the three anonymous reviewers for their very helpful and invaluable suggestions on this manuscript.

Conflicts of Interest: The authors declare no conflicts of interest.

References

1. Hein, S. Knot attributes and occlusion of naturally pruned branches of *Fagus sylvatica*. *For. Ecol. Manag.* **2008**, *256*, 2046–2057. [[CrossRef](#)]
2. Montagu, K.D.; Kearney, D.E.; Smith, R.G.B. The biology and silviculture of pruning planted eucalypts for clear wood production—A review. *For. Ecol. Manag.* **2003**, *179*, 1–13. [[CrossRef](#)]
3. Maguire, D.A.; Kershaw, J.R.; Hann, D.W. Predicting the effects of silvicultural regime on branch size and crown wood core in Douglas-fir. *For. Sci.* **1991**, *37*, 1409–1428.

4. Roeh, R.L.; Maguire, D.A. Crown profile models based on branch attributes in coastal Douglas-fir. *For. Ecol. Manag.* **1997**, *96*, 77–100. [[CrossRef](#)]
5. Karaszewski, Z.; Bembenek, M.; Mederski, P.S.; Szczepanska-Alvarez, A.; Byczkowski, R.; Kozłowska, A.; Michnowicz, K.; Przytula, W.; Giefing, D.F. Identifying beech round wood quality-distribution of beech timber qualities and influencing defects. *Drewno. Pr. Nauk. Donies. Komunik.* **2013**, *56*, 39–54.
6. Macdonald, E.; Hubert, J. A review of the effects of silviculture on timber quality of *Sitka spruce*. *Forestry* **2002**, *75*, 107–138. [[CrossRef](#)]
7. Shigo, A.L. Compartmentalization: A conceptual framework for understanding how trees grow and defend themselves. *Annu. Rev. Phytopathol.* **1984**, *22*, 189–214. [[CrossRef](#)]
8. O'Hara, K.L. Pruning wounds and occlusion: A long-standing conundrum in forestry. *J. For.* **2007**, *105*, 131–138.
9. Kicki, J. Effects of initial spacing on the stem and branch properties and graded quality of *Picea abies* (L.) karst. *Scand. J. For. Res.* **1992**, *7*, 12.
10. Mäkinen, H.; Song, T. Evaluation of models for branch characteristics of Scots pine in Finland. *For. Ecol. Manag.* **2002**, *158*, 25–39. [[CrossRef](#)]
11. Beaulieu, E.; Schneider, R.; Berninger, F.; Ung, C.H.; Swift, D.E. Modeling jack pine branch characteristics in Eastern Canada. *For. Ecol. Manag.* **2011**, *262*, 1748–1757. [[CrossRef](#)]
12. Hein, S.; Mäkinen, H.; Yue, C.; Kohnle, U. Modelling branch characteristics of Norway spruce from wide spacing in Germany. *For. Ecol. Manag.* **2007**, *242*, 155–164. [[CrossRef](#)]
13. Smith, R.G.B.; Dingle, J.; Kearney, D.; Montagu, K. Branch occlusion after pruning in four contrasting sub-tropical eucalypt species. *J. Trop. For. Sci.* **2006**, *18*, 117–123.
14. Wang, C.S.; Hein, S.; Zhao, Z.G.; Guo, J.J.; Zeng, J. Branch occlusion and discoloration of *Betula alnoides* under artificial and natural pruning. *For. Ecol. Manag.* **2016**, *375*, 200–210. [[CrossRef](#)]
15. Chen, L.; Zeng, J.; Jia, H.Y.; Zeng, J.; Guo, W.F.; Cai, D.X. Growth and nutrient uptake dynamics of *Mytilaria laosensis* seedlings under exponential and conventional fertilizations. *Soil Sci. Plant Nutr.* **2012**, *58*, 618–626. [[CrossRef](#)]
16. Guo, W.F.; Cai, D.X.; Jia, H.Y.; Li, Y.X.; Lu, Z.F. Growth laws of *Mytilaria laosensis* plantation. *For. Res.* **2006**, *19*, 585.
17. Huang, Z.T.; Wang, S.F.; Jiang, Y.M.; Mo, J.X. Exploitation and utilization prospects of eximious native tree species *Mytilaria laosensis*. *J. Guangxi Agric. Sci.* **2009**, *40*, 1220–1223.
18. Wang, Z.H.; Yin, G.T.; Yang, J.C.; Qin, G.M. Effects of different density on branch development of *Mytilaria laosensis*. *For. Res.* **2019**, *32*, 78–86.
19. Dănescu, A.; Ehring, A.; Bauhus, J.; Albrecht, A.; Hein, S. Modelling discoloration and duration of branch occlusion following green pruning in *Acer pseudoplatanus* and *Fraxinus excelsior*. *For. Ecol. Manag.* **2015**, *335*, 87–98. [[CrossRef](#)]
20. Pinheiro, J.; Bates, D. *Mixed-Effects Models in S and S-PLUS*; Springer Science and Business Media: Berlin, Germany, 2006.
21. Stewart, G.W. Collinearity and least squares regression. *Stat. Sci.* **1987**, *2*, 68–84. [[CrossRef](#)]
22. Nakagawa, S.; Schielzeth, H. A general and simple method for obtaining R^2 from generalized linear mixed effects models. *Methods Ecol. Evol.* **2013**, *4*, 133–142. [[CrossRef](#)]
23. Pepe, M.S. Receiver operating characteristic methodology. *J. Am. Stat. Assoc.* **2000**, *95*, 308–311. [[CrossRef](#)]
24. Zhang, S.; Chauret, G.; Duchesne, I.; Schnelder, R. *Maximizing the Value of Jack Pine Resource*; Technical Report; Forintek Canada Corp: Quebec, QC, Canada, 2005.
25. Wang, C.; Zhao, Z.; Hein, S.; Zeng, J.; Schuler, J.; Guo, J.J.; Zeng, J. Effect of planting density on knot attributes and branch occlusion of *Betula alnoides* under natural pruning in southern China. *Forests* **2015**, *6*, 1343–1361. [[CrossRef](#)]
26. Moberg, L. Models of internal knot diameter for *Pinus sylvestris*. *Scand. J. For. Res.* **2000**, *15*, 177–187. [[CrossRef](#)]
27. Moberg, L. Models of internal knot properties for *Picea abies*. *For. Ecol. Manag.* **2001**, *147*, 123–138. [[CrossRef](#)]
28. Trincado, G.; Burkhart, H.E. A framework for modeling the dynamics of first-order branches and spatial distribution of knots in Loblolly pine trees. *Can. J. For. Res.* **2009**, *39*, 566–579. [[CrossRef](#)]
29. Mäkinen, H. Effect of intertree competition on branch characteristics of *Pinus sylvestris* families. *Scand. J. For. Res.* **1996**, *11*, 129–136. [[CrossRef](#)]

30. Sandi, M.; Sandi, W.; Nicolescu, V.N. Wood discoloration in relation to wound size in northern red oak (*Quercus rubra* L.) trees subject to artificial pruning. *Span. J. Rural Dev.* **2012**, *3*, 53–60. [[CrossRef](#)]
31. Maurin, V.; DesRochers, A. Physiological and growth responses to pruning season and intensity of hybrid poplar. *For. Ecol. Manag.* **2013**, *304*, 399–406. [[CrossRef](#)]
32. Hevia, A.; Álvarez-González, J.G.; Majada, J. Comparison of pruning effects on tree growth, productivity and dominance of two major timber conifer species. *For. Ecol. Manag.* **2016**, *374*, 82–92. [[CrossRef](#)]
33. Hein, S.; Spiecker, H. Comparative analysis of occluded branch characteristics for *Fraxinus excelsior* and *Acer pseudoplatanus* with natural and artificial pruning. *Can. J. For. Res.* **2007**, *37*, 1414–1426. [[CrossRef](#)]
34. Nicolescu, V.N.; Sandi, M.; Păun, M. Occlusion of pruning wounds on northern red oak (*Quercus rubra*) trees in Romania. *Scand. J. For. Res.* **2013**, *28*, 340–345. [[CrossRef](#)]
35. O'Hara, K.L.; Buckland, P.A. Prediction of pruning wound occlusion and defect core size in ponderosa pine. *West. J. Appl. For.* **1996**, *11*, 40–43. [[CrossRef](#)]
36. Petrucio, M.; Briggs, D.; Barbour, R.J. Predicting pruned branch stub occlusion in young, coastal Douglas-fir. *Can. J. For. Res.* **1997**, *27*, 1074–1082. [[CrossRef](#)]
37. Forrester, D.I.; Baker, T.G. Growth responses to thinning and pruning in *Eucalyptus globulus*, *Eucalyptus nitens*, and *Eucalyptus grandis* plantations in southeastern Australia. *Can. J. For. Res.* **2011**, *42*, 75–87. [[CrossRef](#)]
38. Forrester, D.I.; Collopy, J.J.; Beadle, C.L.; Warren, C.R.; Baker, T.G. Effect of thinning, pruning and nitrogen fertiliser application on transpiration, photosynthesis and water-use efficiency in a young *Eucalyptus nitens* plantation. *For. Ecol. Manag.* **2012**, *266*, 286–300. [[CrossRef](#)]
39. Hein, S.; Collet, C.; Ammer, C.; Goff, N.L.; Skovsgaard, J.P.; Savill, P. A review of growth and stand dynamics of *Acer pseudoplatanus* L. in Europe: Implications for silviculture. *Forestry* **2008**, *82*, 361–385. [[CrossRef](#)]
40. Day, M.E.; Greenwood, M.S.; Diaz-Sala, C. Age- and size-related trends in woody plant shoot development: Regulatory pathways and evidence for genetic control. *Tree Physiol.* **2002**, *22*, 507–513. [[CrossRef](#)]
41. Schwarze, F.; Engels, J.; Mattheck, C. Holzersetzende Pilze in Bäumen. *Strategien der Holzersetzung Rombach Ökologie* **1999**, *5*.
42. Wardlaw, T.J.; Neilsen, W.A. Decay and other defects associated with pruned branches of *Eucalyptus nitens*. *Tasforests Hobart* **1999**, *11*, 49–58.
43. Beadle, C.; Barry, K.; Hardiyanto, E.; Irianto, R.; Mohammed, C.; Rimbawanto, A. Effect of pruning *Acacia mangium* on growth, form and heart rot. *For. Ecol. Manag.* **2007**, *238*, 261–267. [[CrossRef](#)]
44. Barry, K.M.; Pearce, R.B.; Mohammed, C.M. Properties of reaction zones associated with decay from pruning wounds in plantation grown *Eucalyptus nitens*. *For. Pathol.* **2000**, *30*, 233–245. [[CrossRef](#)]
45. Lonsdale, D.; Pautasso, M.; Holdenrieder, O. Wood-decaying fungi in the forest: Conservation needs and management options. *Eur. J. For. Res.* **2008**, *127*, 1–22. [[CrossRef](#)]
46. Barry, K.M.; Irianto, R.S.B.; Tjahjono, B.; Tarigan, M.; Agustini, L.; Hardiyanto, E.B.; Mohammed, C.L. Variation of heart rot, sap wood infection and polyphenol extractives with provenance of *Acacia mangium*. *For. Pathol.* **2006**, *36*, 183–197. [[CrossRef](#)]

